FEBS Letters 484 (2000) 224–228 FEBS 24267

The roles of Glu93 and Tyr149 in astacin-like zinc peptidases

Irene Yiallouros*, Eva Große Berkhoff, Walter Stöcker

Institute of Zoophysiology, University of Münster, Hindenburgplatz 55, D-48143 Münster, Germany

Received 9 October 2000; accepted 13 October 2000

First published online 26 October 2000

Edited by Hans Eklund

Abstract The catalytic zinc of astacin, a prototype of the astacin family and the metzincin superfamily of metalloproteinases is coordinated by three histidines, a glutamate bound water and a tyrosine. In order to assess the roles of active site key residues, two mutants, Glu93Ala-astacin and Tyr149Phe-astacin, were expressed in *Escherichia coli*, affinity-purified and renatured. While the Glu93Ala mutant was inactive, the Tyr149Phe mutant retained about 2.5% residual activity toward Dns-Pro-Lys-Arg*Ala-Pro-Trp-Val, based on the k_{cat}/K_m value for recombinant wild-type astacin. These results support a model in which Glu93 is the general base in substrate hydrolysis, whereas Tyr149 contributes to transition state binding.

Key words: Astacin; Astacin family; Metzincin; Catalytic mechanism; Site-directed mutagenesis

1. Introduction

The collagenolytic zinc endopeptidase astacin of the crayfish *Astacus astacus* L. is the prototype of the astacin family [1–3] and the metzincin superfamily [4,5]. The physiological roles of these proteases, which include the BMP1/Tolloid-like enzymes [6–9], hatching proteases [10,11] and the meprins [12–14], are ranging from food digestion to functions during embryonic development and tissue differentiation.

The catalytic zinc ion in the active center of astacin is coordinated by three histidine residues (His92, His96 and His102), one glutamic acid (Glu93) bridged water molecule and a tyrosine residue (Tyr149; Fig. 1) [15]. While the histidine ligands and the glutamic acid residue are part of the zinc binding consensus sequence HExxHxxGxxH, the tyrosine ligand is located in a conserved motif, the Met-turn, containing an invariant methionine residue (Met147; Fig. 1) [4]. Beside the extended zinc binding motif, this Met-turn is a key feature of metzincin-type peptidases, namely the adamalysins/reprolysins/ADAMs (ADAM = A Disintegrin And Metalloproteinase), the matrixins and the serralysins. Among these, only the serralysins and the astacins contain a tyrosine residue as a fifth zinc ligand [4].

When the three-dimensional structure of astacin was elucidated [15], the observation of this fifth metal ligand raised the question about its function, since the coordination sphere of the zinc ion seemed to be overcrowded by five ligands already in the absence of a substrate [2]. Hence, it was proposed that a rearrangement of Tyr149 should be necessary for substrate binding and catalysis [2]. This assumption was confirmed by X-ray crystal structure analysis of astacin complexed with a transition state analogue inhibitor [16]. In this complex the critical Tyr149 had moved by rotation around its backbone into a position 0.5 nm (5 Å) removed from the zinc ion which was now coordinated by the inhibitor's phosphinyl group mimicking the tetracoordinated carbon during substrate turnover. The tyrosyl hydroxyl being in hydrogen bonding distance to one of the phosphinyl oxygens. This scenario of a 'tyrosine switch' during substrate binding suggested a role for this tyrosine residue in transition state stabilization [16], which appeared in accordance with earlier observations on the neutral peptidases thermolysin and carboxypeptidase A [17–19]. There His231 (thermolysin) [18] and Arg127 (carboxypeptidase A) [17,19] form hydrogen bonds to transition state analogue phosphonyl oxygens and can be considered as counterparts of Tyr149 in astacin. However, in contrast to Tyr149 (Ast), His231 (TL) and Arg127 (CPA) are not involved in zinc coordination. Replacement of His231 in a thermolysin-like *Bacillus* neutral protease results in a mutant with reduced activity [20], supporting the function of this residue in transition state stabilization during catalysis.

The active sites of astacin and the thermolysin-like enzymes are topologically similar [4,5]. They have in common the short zinc binding sequence HExxH, but in contrast to the pentacoordinated zinc ion of the astacins, the metal in these neutral peptidases is tetrahedrally coordinated by only four ligands including one glutamic acid residue (Glu166, His142, His146 and one water molecule), hence the designation gluzincins [21]. In thermolysin, Glu143 (corresponding to Glu93 of astacin) included in the HExxH motif is thought to act as the general base during catalysis, which transfers a proton from the catalytic water to the amide of the scissile peptide bond. However, an alternative mechanism has been discussed recently for thermolysin-like metallopeptidases [22] and for serralysins [23], attributing the role of the general base to His231 in thermolysin and Tyr216 in serralysin, respectively. Mutagenesis studies on astacin or serralysin, which could shed light on the role of the critical glutamate and tyrosine residues in their active sites, have been lacking so far.

In order to clarify the role of the tyrosine residue in astacin-like enzymes, we used site-directed mutagenesis to substitute active site key residues by non-functional ones. The mutants Tyr149Phe-astacin and Glu93Ala-astacin were expressed in

*Corresponding author. Fax: (49)-251-8321766.
E-mail: yiallou@uni-muenster.de

Abbreviations: Dns, 5-(dimethylamino)-naphthalene-1-sulfonyl; NTA, nitrilotriacetic acid; IPTG, isopropyl β-D-thiogalactopyranoside; GuHCl, guanidine hydrochloride; PAGE, polyacrylamide gel electrophoresis; Ψ, indicates replacement of the peptide bond by the group given in parentheses

0014-5793/00/$20.00
PII: S0014-5793(00)02163-3

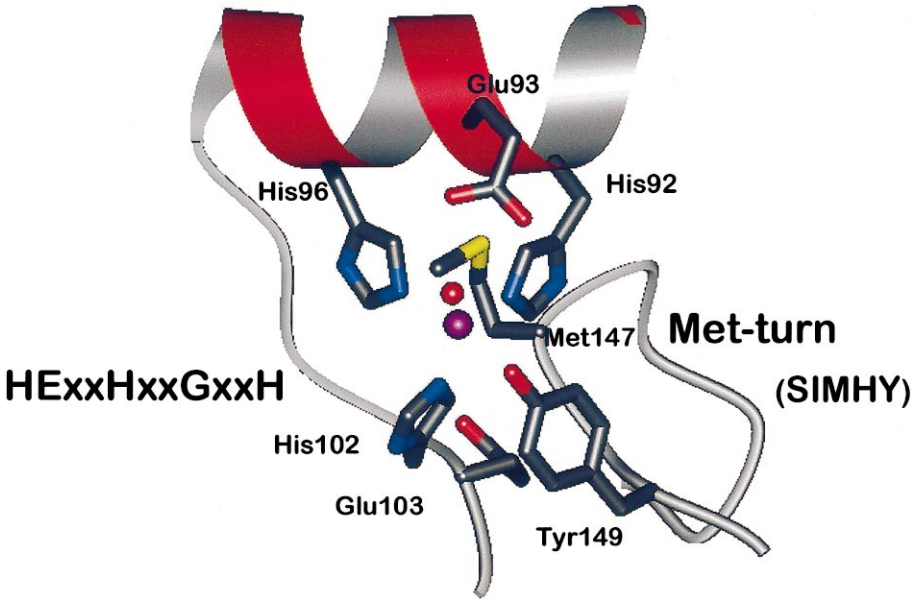

Fig. 1. The active site zinc ion (magenta) of astacin is trigonal bipyramidally coordinated by three histidine residues, a water molecule (red) and a tyrosine residue [15]. His92, His96, His102 and the water-linked Glu93 are part of the consensus sequence HExxHxxGxxH. Tyr149 is located in the conserved Met-turn motif, named after the depicted methionine residue (Met147). Molscript [31] was used for modelling.

Escherichia coli cells, purified and renatured. We show that the Glu93Ala mutant is catalytically inactive and the Tyr149-Phe mutant is 40-fold less active than the wild-type enzyme.

2. Materials and methods

2.1. Site-directed mutagenesis

Site specific mutagenesis of the recombinant wild-type astacin [24] was performed using the 'ExSite™ PCR-based site-directed mutagenesis kit' (Stratagene, Heidelberg, Germany). The mutations were introduced with the 5′-phosphorylated (Ph) primers (TIB MOLBIOL, Berlin, Germany): Tyr149Phe-sense 5′-Ph-ATGCAC**TTC**GGCAAGTACTCCTTCTCCATACAG; Tyr149Phe-antisense 5′-Ph-TATGCTGTAGT ACTGGTAATCCT CACCCACATAGCG; Glu93Ala-sense 5′-Ph- **GCG**CTCATGCATGCCATTGGCTTC; Glu93Ala-antisense 5′-Ph-ATGGATGATGGTGCCATGGTAAACACAACC.

The sense primers were carrying the respective changed triplet (underlined). Sense and antisense primers bind to their cognate cDNA strands, thereby not overlapping, but bordering on each other.

The following amplification of the whole plasmid was performed in a thermocycler (Hybaid, Middlesex, UK) using one cycle (i) 94°C (4 min), 52°C (2 min), 72°C (2 min), 12 cycles (ii) 94°C (1 min), 58°C (2 min), 72°C (1 min); and one cycle (iii) 72°C (5 min).

Epicurian Coli® XL1-Blue supercompetent cells (included in the kit) were transformed with the resulting circular plasmids pET3a-Y149F-astacin and pET3a-E93A-astacin. Both sequences were confirmed by DNA sequencing (SeqLab, Göttingen, Germany).

2.2. Protein expression

The recombinant astacins were expressed for 4 h by *E. coli* BL21(DE3) cells grown at 37°C to an optical density of 0.7–0.9 at 600 nm, after induction with 0.4 mM IPTG (isopropyl β-D-thiogalactopyranoside) as described [24]. The overexpressed protein is deposited in the form of inclusion bodies in the cytoplasm.

2.3. Protein purification and renaturation

2.3.1. Nickel nitrilotriacetic acid (Ni-NTA) affinity chromatography. 3.5 g bacteria cell pellet was mixed with 50 μl β-mercaptoethanol for 3 min before adding 5×1 ml lysis buffer (6 M guanidine hydrochloride (GuHCl), 0.1 M NaH_2PO_4, 0.01 M Tris–HCl, pH 8.0, 1 μM pepstatin, 2 μM *trans*-epoxysuccinyl-L-leucylamido-4-guanidino butane (E64), 500 μM phenylmethylsulfonyl fluoride) and followed by a 60 min incubation under stirring. Another 30 ml lysis buffer was added and the mixture was further incubated for 30 min. After centrifugation (15 min at 10 000×*g*), the supernatant was applied to a Ni-NTA affinity column (Qiagen, Hilden, Germany). The column was subsequently washed with 6 M GuHCl, 0.1 M NaH_2PO_4, 0.01 M Tris–HCl, pH 8.0. Further washing of the column was performed with the same buffer by stepwise lowering the pH value to 6.3 and 5.9. Final elution was achieved at pH 4.5.

2.3.2. Protein renaturation. Renaturation after Ni-NTA affinity chromatography was achieved by diluting the protein to a concentration of 10 μg/ml into 50 mM Tris–HCl buffer pH 8.0, containing 0.8 M L-arginine, 0.1 mM oxidized glutathione, 1 mM reduced glutathione [24], and 1 mM Pro-Leu-Gly-NHOH followed by incubation for 24 h at 4°C. Finally the protein solution was dialyzed against 50 mM Tris–HCl buffer pH 7.0 in the presence of 10 μM $ZnSO_4$.

2.3.3. Pro-Leu-Gly-NHOH affinity chromatography [25]. Renatured proteins were applied to a Pro-Leu-Gly-hydroxamate affinity column, equilibrated with 50 mM Tris–HCl buffer pH 7.0 [23]. The column was washed with 0.1 M Tris–HCl pH 8.0, 0.5 M NaCl and then eluted with 0.1 M Tris buffer/0.5 M NaCl. For neutralization of the high pH value due to the elution buffer, the fractions were collected in an equal volume of 0.3 M Tris–HCl buffer pH 7.5.

2.4. Sodium dodecyl sulfate–polyacrylamide gel electrophoresis (SDS–PAGE) and Western blot analysis

SDS–PAGE was performed according to standard procedures in 14% polyacrylamide gels. In the case of samples containing GuHCl, a trichloro acetic acid precipitation was performed prior to electrophoresis according to the protocol of Qiagen (Hilden, Germany). Coomassie brilliant blue G250 was used for background free gel staining [26].

Proteins were blotted onto PVDF (polyvinylidene difluoride) membranes using a semi-dry blotting apparatus (Phero-Multiblot tMUL-100, Biotech Fischer). The membranes were blocked by 2 h incubation with 5% low fat milk powder in TBS buffer pH 7.4. Polyclonal rabbit anti-astacin antiserum, preabsorbed with BL21(DE3)pET3a total cell extract, was used for immunodetection of the transferred proteins. The second antibody (goat anti-rabbit, coupled with horseradish peroxidase) was added after incubation for 2 h at room temperature and washing with TBS buffer. The ECL Western blot detection kit (Amersham Life Sciences, Braunschweig, Germany) was used for the chemiluminescent substrate reaction according to the manufacturer's manual.

2.5. Gelatin zymography

SDS–PAGE gels containing 0.1% gelatin were used for enzyme activity assays.

After electrophoresis, the gel was washed 1 h with 2.5% Triton X-100 followed by 16 h incubation in 0.05 M Tris–HCl pH 7.5/0.2 M NaCl/0.005 M $CaCl_2$. Uncolored spots localize proteolytic activity on the Coomassie brilliant blue G250-stained gels.

2.6. Enzyme kinetics

Enzyme activity was determined with a Luminescence Spectrometer LS 50 (Perkin-Elmer) using the quenched fluorescent substrate 5-(dimethylamino)-naphthalene-1-sulfonyl (Dns)-Pro-Lys-Arg-Ala-Pro-Trp-Val [27]. Assays were performed in 0.1 M Tris–HCl buffer pH 8.0 in a total volume of 400 μl (excitation at 280 nm, emission at 350 nm).

The kinetic parameters k_{cat}, K_m and k_{cat}/K_m were calculated by directly fitting the data to the Michaelis–Menten equation using GraFit 4.0 (Erithacus Software Ltd., Staines, UK).

3. Results

3.1. Site specific mutagenesis and bacterial protein expression

Two mutants were created, based on the plasmid pET3a-astacin [24], containing the cDNA of the mature astacin fused with a C-terminal tag of five histidine residues (His-tag) to be used for subsequent affinity purification. In order to investigate the function of Glu93 and Tyr149, both residues were replaced by a PCR-based mutagenesis by alanine and phenylalanine, respectively. The resulting circular plasmids containing the point mutations were verified by sequencing and used to transform *E. coli* BL21(DE3) cells (not shown). Protein expression was induced after the cells were grown to an optical density of $A_{600nm} = 0.7–0.9$ by addition of 0.4 mM IPTG, leading to the formation of inclusion bodies containing the proteins of interest.

3.2. Protein purification and renaturation

As the overexpressed proteins were deposited in the form of inclusion bodies in the cytoplasm, they had to be solubilized using GuHCl and β-mercaptoethanol. The whole bacterial cell extract was then submitted to a Ni-NTA affinity chromatography. Like recombinant wild-type astacin, the astacin variants were eluted in a single peak at pH 4.5. The pooled fractions were renatured in the presence of Pro-Leu-Gly-NHOH (a competitive inhibitor of astacin) before applying them to a Pro-Leu-Gly-NHOH affinity column [24]. Under these conditions, only enzyme molecules with a correctly folded active site bind to the column [14,24]. Each of the selectively separated renatured astacin variants was collected in a single peak, respectively, which was resolved as a distinct band in SDS–PAGE and Western blot analysis (Fig. 2). The recombinant astacins have a higher molecular mass (M_r 23 581) compared to the crayfish enzyme (M_r 22 614), due to the His-tag. Recombinant wild-type astacin treated in the same way as the mutants was used as a standard.

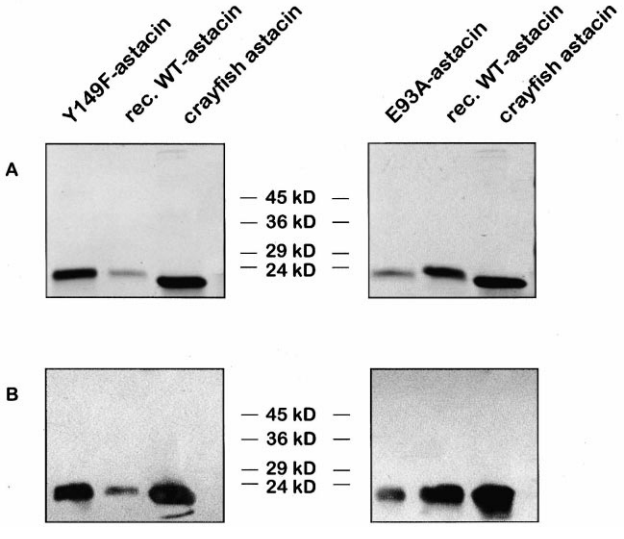

Fig. 2. Coomassie brilliant blue-stained 14% SDS–PAGE gel (A) and Western blot analysis (B) of Y149F-astacin (3 μg) and E93A-astacin (1.3 μg). Recombinant wild-type (WT) astacin (2 μg) is shown in comparison to the mutants. Crayfish astacin (5 μg) is used as a standard. The higher molecular weight of the recombinant astacins is due to their His-tag. Polyclonal anti-astacin antiserum was used for immunodetection.

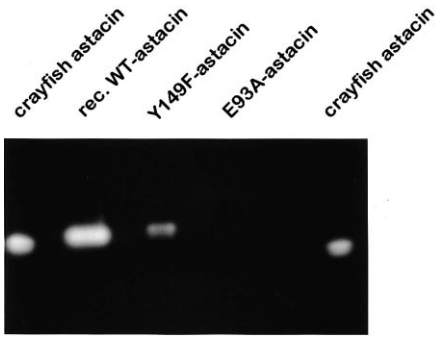

Fig. 3. Proteolytic activity of the recombinant astacin variants is shown by digestion of immobilized gelatin (0.1%) in a 14% SDS–PAGE gel, stained with Coomassie brilliant blue. Y149F-astacin (20 ng) is less active compared to recombinant wild-type (WT) astacin (20 ng). No activity is detectable for E93A-astacin (20 ng). Crayfish astacin is shown as a standard (left lane 10 ng, right lane 5 ng).

3.3. Enzyme activity

Gelatin zymography was used to qualitatively analyze the proteolytic activity of the astacin variants. After Pro-Leu-Gly-NHOH affinity chromatography, recombinant Y149F-astacin, but not E93A-astacin, shows proteolytic degradation of gelatin (Fig. 3). Compared to the recombinant wild-type enzyme, the Y149F-astacin proved to be less active. All three variants were loaded at identical concentrations.

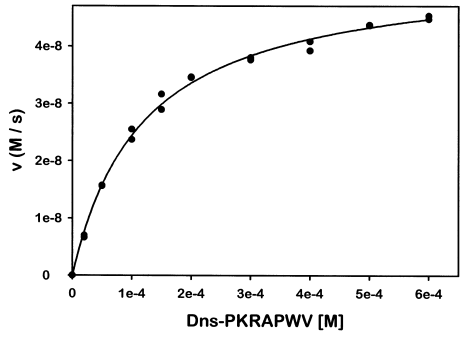

Fig. 4. The Michaelis–Menten diagram shows the hydrolysis of Dns-PKRAPWV by 1×10^{-7} M Y149F-astacin (in 0.1 M Tris–HCl buffer pH 8.0 at 25°C). The kinetic parameters for cleavage of the fluorescent substrate are calculated with $K_m = 1.2 \times 10^{-4}$ M, $k_{cat} = 0.54$ s^{-1} and $k_{cat}/K_m = 4.5 \times 10^{-3}$ M^{-1} s^{-1}.

Table 1
Kinetic analysis of recombinant wild-type astacin and astacin mutants

Astacin variant (M)	K_m (M)	k_{cat} (s^{-1})	k_{cat}/K_m (M^{-1} s^{-1})	Substrate (M)
Wild-type astacin (1×10^{-9})	3.2×10^{-4}	57.86	1.81×10^{5}	5×10^{-6}–1×10^{-3}
Y149F-astacin (1×10^{-7})	1.2×10^{-4}	0.54	4.5×10^{3}	2×10^{-6}–6×10^{-4}
E93A-astacin (3.5×10^{-7})	no detectable activity			5×10^{-4}–1×10^{-3}

The enzyme concentrations and the substrate ranges used in the assays are indicated. The enzymatic substrate cleavage was monitored at 25°C in 0.1 M Tris–HCl buffer pH 8.0. Based on the k_{cat}/K_m value for recombinant wild-type astacin, the Y149F-astacin retains an activity of about 2.5%. For E93A-astacin no activity was detectable.

3.4. Enzyme kinetics

To quantify the enzymatic activity of the astacin mutants and to analyze the influence of substituting the residues Glu93 and Tyr149 on substrate binding and catalysis, a fluorimetric assay was carried out. Determination of the kinetic parameters K_m, k_{cat} and k_{cat}/K_m was performed for the hydrolysis of the fluorescent substrate Dns-Pro-Lys-Arg-Ala-Pro-Trp-Val by wild-type and mutant astacins. This peptide is one of the most sensitive substrates known for astacin [27]. Compared to recombinant wild-type astacin, the Y149F mutant shows a 40-fold drop of the k_{cat}/K_m value (from 1.8×10^{5} M^{-1} s^{-1} to 4.5×10^{3} M^{-1} s^{-1}, respectively), while E93A-astacin proved to be inactive (Fig. 4, Table 1). The reduced activity of Y149F-astacin is mainly due to a decrease of k_{cat}, and the corresponding K_m (1.2×10^{-4} M) is only about one third of the value determined for the recombinant wild-type enzyme ($K_m = 3.2\times10^{-4}$ M).

4. Discussion

In the proposed mechanism of substrate hydrolysis by the zinc endopeptidase astacin, Glu93 was suggested previously to act as the general base, responsible for the polarization of the catalytic water molecule and proton transfer from this water molecule to the amide group of the scissile peptide bond [16]. It has been proposed also that the zinc ligand Tyr149 assists in catalysis by stabilizing the transition state during peptide hydrolysis.

To prove this hypothesis, site-directed mutagenesis was used to substitute two key residues in the active center of astacin by non-functional ones. The mutants Tyr149Phe-astacin and Glu93Ala-astacin were expressed, purified and folded.

As recently described [24], Pro-Leu-Gly-NHOH affinity chromatography is an effective method to discriminate between correctly folded astacin molecules and unfolded forms. The hydroxamate Pro-Leu-Gly-NHOH is a competitive inhibitor of astacin [16]. It complexes the zinc ion in the catalytic center and aligns in an antiparallel manner along the so-called edge strand forming the rim of the active site cleft. Both mutants bind to this column in the same manner as the wild-type protein, a strong indication for their native-like fold. It has been shown also that amino-terminally extended proforms of the astacin-like proteases like human promeprin only bind to Pro-Leu-Gly-NHOH after removal of the propeptide [14]. This is further evidence that binding to this inhibitor is a good indication for a correct conformation and accessibility of the active site.

The consequence of replacing the residues Glu93 and Tyr149 was demonstrated in activity assays. The Glu93Ala mutant is inactive in both, gelatin zymography and toward the fluorescent substrate Dns-Pro-Lys-Arg*Ala-Pro-Trp-Val, the best astacin substrate known so far [27]. This supports the essential role of Glu93 as the general base during catalysis. Interestingly, the substitution of the critical Glu198 residue in matrilysin resulted in an enzyme species displaying still residual activity albeit about 2000-fold less than the wild-type protease [28]. In these experiments, the Glu198Ala mutant of matrilysin was assayed at a 42-fold higher concentration as the wild-type enzyme [28]. For comparison, in the case of astacin, the concentration of the Glu93Ala mutant used for activity assays was 350-fold higher than the wild-type standard. Even under these conditions there was no activity detectable.

The Tyr149Phe mutant retains a reduced activity, which is mainly due to an about 100-fold decrease of k_{cat}. The decrease to about one third of the K_m value of the mutant compared to the recombinant wild-type enzyme is probably due to the lacking hydroxyl group of the substituted residue and hence to the missing ability to provide a hydrogen bond. The activity of the Tyr149Phe mutant indicates that Tyr149 is not indispensable for catalysis. But its importance for catalysis is shown by the fact that its presence enhances catalysis about 40-fold (k_{cat}/K_m). Therefore Tyr149 is probably responsible for the stabilization of the transition state during substrate hydrolysis, as previously proposed by [16]. The position of Tyr149 in the X-ray structure of astacin complexed with a phosphinic transition state analogue is in agreement with this function. Hence, the tyrosine switch mechanism implies the opening of a gap between the tyrosine phenolic group and the zinc ion into which the inhibitor's phosphinyl group is inserted. The distance of 0.27 nm between the hydroxyl group of Tyr149 and one lower oxygen of the phosphinyl group's oxygen atoms (mimicking the transition state of the scissile peptide bond) enables the formation of a hydrogen bond [16]. The participation of Tyr149 in substrate binding is also indicated by the Cu(II)-astacin absorption spectrum. As shown previously, the spectrum of free Cu(II)-astacin shows two intense absorption maxima at 445 nm and 325 nm, indicative of oxygen–metal charge transfer between the tyrosine phenol group and the metal [29]. Upon addition of the phosphonamidate inhibitor Z-FΨ(PO_2NH)APF to Cu(II)-astacin, we observed a decrease of both of these spectral maxima (unpublished results), indicating that the interaction of the phenolic oxygen with the metal ion in the catalytic center is interrupted. The same result was reported recently for copper astacin from *Procambarus* spp. [30].

The data presented here strongly support the hypothesis that Tyr149 of astacin is involved in substrate binding and in stabilization of the transition state during catalysis, while the role of the general base is played by Glu93.

Acknowledgements: This work was supported by the Deutsche Forschungsgemeinschaft to (Sto 185/3-2).

References

[1] Dumermuth, E., Sterchi, E.E., Jiang, W.P., Wolz, R.L., Bond, J.S., Flannery, A.V. and Beynon, R.J. (1991) J. Biol. Chem. 266, 21381–21385.
[2] Stöcker, W., Gomis-Rüth, F.-X., Bode, W. and Zwilling, R. (1993) Eur. J. Biochem. 214, 215–231.
[3] Bond, J.S. and Beynon, R.J. (1995) Prot. Sci. 4, 1247–1261.
[4] Bode, W., Gomis-Rüth, F.-X. and Stöcker, W. (1993) FEBS Lett. 331, 134–140.
[5] Stöcker, W. and Bode, W. (1995) Curr. Opin. Struct. Biol. 5, 383–390.
[6] Kessler, E., Takahara, K., Biniaminov, L., Brusel, M. and Greenspan, D.S. (1996) Science 271, 360–362.
[7] Li, S.W., Sieron, A.L., Fertala, A., Hojima, Y., Arnold, W.V. and Prockop, D.J. (1996) Proc. Natl. Acad. Sci. USA 93, 5127–5130.
[8] Scott, I.C., Blitz, I.L., Pappano, W.N., Imamura, Y., Clark, T.G., Steiglitz, B.M., Thomas, C.L., Maas, S.A., Takahara, K., Cho, K.W.Y. and Greenspan, D.S. (1999) Dev. Biol. 213, 283–300.
[9] Blader, P., Rastegar, S., Fischer, N. and Strähle, U. (1997) Science 278, 1937–1940.
[10] Geier, G. and Zwilling, R. (1998) Eur. J. Biochem. 253, 796–803.
[11] Yasumasu, S., Yamada, K., Akasaka, K., Mitsunage, K., Iuchi, I., Shimada, H. and Yamigami, K. (1992) Dev. Biol. 153, 250–258.
[12] Sterchi, E.E., Naim, H.Y., Lentze, M.J., Hauri, H.P. and Fransen, J.A. (1988) Arch. Biochem. Biophys. 265, 105–118.
[13] Beynon, R.J., Shannon, J.D. and Bond, J.S. (1981) Biochem. J. 199, 591–598.
[14] Köhler, D., Kruse, M.N., Stöcker, W. and Sterchi, E.E. (2000) FEBS Lett. 465, 2–7.
[15] Bode, W., Gomis-Rüth, F.-X., Huber, R., Zwilling, R. and Stöcker, W. (1992) Nature 358, 164–167.
[16] Grams, F., Dive, V., Yiotakis, A., Yiallouros, I., Vassiliou, S., Zwilling, R., Bode, W. and Stöcker, W. (1996) Nat. Struct. Biol. 3, 671–675.
[17] Auld, D.S. and Vallee, B.L. (1987) in: Hydrolytic Enzymes (Neuberger, A. and Brocklehurst, K., Eds.), pp. 201–255, Elsevier, Amsterdam.
[18] Matthews, B.W. (1988) Acc. Chem. Res. 21, 333.
[19] Christianson, D.W. and Lipscomb, W.N. (1989) Chem. Res. 22, 62–69.
[20] Beaumont, A., O'Donohue, M.J., Paredes, N., Rousselet, N., Assicot, M., Bohuon, C., Fournié-Zaluski, M.-C. and Roques, B.P. (1995) J. Biol. Chem. 270, 16803–16808.
[21] Hooper, N.M. (1994) FEBS Lett. 354, 1–6.
[22] Mock, W.L. and Aksamawati, M. (1994) Biochem. J. 302, 57–68.
[23] Mock, W.L. and Yao, J. (1997) Biochemistry 36, 4949–4958.
[24] Reyda, S., Jacob, E., Zwilling, R. and Stöcker, W. (1999) Biochem. J. 344, 851–857.
[25] Moore, W.M. and Spilburg, C.A. (1986) Biochemistry 25, 5189–5195.
[26] Neuhoff, V. (1990) Biol. Chem. Hoppe-Seyler 371, 10–11.
[27] Stöcker, W., Ng, M. and Auld, D.S. (1990) Biochemistry 29, 10418–10425.
[28] Cha, J. and Auld, D.S. (1997) Biochemistry 36, 16019–16024.
[29] Gomis-Rüth, F.-X., Grams, F., Yiallouros, I., Nar, H., Küsthardt, U., Zwilling, R., Bode, W. and Stöcker, W. (1994) J. Biol. Chem. 269, 17111–17117.
[30] Park, H.I. and Ming, L.-J. (1998) J. Inorg. Biochem. 72, 57–62.
[31] Kraulis, P.J. (1991) J. Appl. Crystallogr. 24, 946–950.